A Comparative Study of CNN-Based Feature Extraction and Machine Learning Classifiers for Identification of Tyre Defect

Festus Orowho and Olufunke Vincent

November 10, 2024

A comparative study of CNN-based feature extraction and machine learning classifiers for identification of tyre defect

Orowho, Festus Oghenekaro
Africa Centre of Excellence on Technology Enhanced Learning,
National Open University,
Abuja, Nigeria.
ace22110013@noun.edu.ng

Vincent, Rebecca Olufunke
Department of Computer Science,
Federal University of Agriculture Abeokuta,
Ogun State, Nigeria
vincentor@funaab.edu.ng

Abstract*—Tyres play a crucial aspect in road safety and vehicle dynamics, as they provide an interface between the vehicle and the road, hence they are very susceptible to fatigue damage during service. In order not to further affect the service life of tyres and automobile safety, tyre manufacturing industries require efficient and accurate methods of detecting defects in tyres during the production process to ensure that defective tyres do not find their way to the market. In this study, we explore the performance of transfer learning using a pre-trained convolutional neural network (CNN) which includes ResNet-50 and VGG-19 for feature extraction, combined with other machine learning algorithms that include Random-forest, Logistic regression, and Support Vector Machine (SVM), for the final classification of the tyre defects. The performance of each of the combined CNN and traditional machine learning algorithms which include ResNet50 + LR, ResNet50 + RF, ResNet50 + SVM, VGG19 + LR, VGG19 + RF, and VGG19 + SVM, are evaluated and compared to other tyre defect classification result in which they combined the algorithm HOG + SVM, LBP + SVM, and HOG + LBP + SVM. The study concludes that VGG19 + LR and VGG19 + SVM methods show promising results for tyre defect detection as they optimise feature representation and classification accuracy.

Keywords*— *convolutional neural network; tyre defect classification; machine learning; deep learning, transfer learning.

I. INTRODUCTION

In the European Union, over 1.3 million road accidents occur yearly resulting in over 40,000 deaths [1]. According to the World Health Organization, 40% of the deaths and people who are disabled from road accidents each year are caused by tyre failures [2], hence to ensure high-quality products, it is necessary to finalise quality inspection during the production stages [3] so that defective tyres do not find their way to the market, to avoid tyre related accident or financial loss from restitution which is estimated at over 100 million dollars per year [4].

During the mass production of tyres, it is difficult to conduct the final quality inspection before they are placed on the market due to the visual and qualitative inspection aspects of the production process which involves high mechanical repetition, and strength and is often carried out in a poor working environment that is not healthy. As a result of the tedious nature of this manual method of inspection, the process tends to be very inaccurate and some tyres that have nominal features may have associated hidden material and geometric defects caused by incorrect production management systems as the rubber material ages, it leads to non-uniformity on tyre-road interaction and reduction in the service life of the tyre as a result of accelerated fatigue damage [5] – [7]. This fatigue damage arises from the fact that while tyres are in service, the polymer-based materials used in the production of the tyre tend to undergo a rise in internal temperature and periodic deformation as a result of kinetic energy built up inside the tyre which is converted into thermal energy that increases the internal temperature of the tyre, causing temperature rise that usually led to the acceleration of the ageing of the rubber material [8].

Like other component defects in automobiles, tyres are susceptible to defects that can compromise the integrity and safety of vehicles, therefore timely detection and repair are crucial for maintaining road safety and preventing potential accidents. Some of the common tyre defects include Bubble and blisters which may arise during production or Bulges caused by impact damage and potholes during service, another defect is Sidewall damage caused by impact, and also tread wear which may occur from improper inflation, misalignment, or suspension issues. Other common defects may include punctures, cuts, and gashes on the tyre surface from a sharp object, Bead damage, Belt Separation, Tyre Ply Separation, and Inner Liner damage [9] – [12]. Currently, most tyre manufacturer uses traditional tyre defect detection methods carried out manually by x-ray imaging which tend to be inefficient, posing a great challenge during defect detection at the production stage [13], and researchers have conducted various experiments to find a more reliable way to improve the operation by using deep learning to automate the process of defect detection [13] – [17].

In a study by Weyssenhoff et al. [10], they analysed selected tyre defects and the causes that may arise during the manufacturing process, they noted that defects relating to non-uniformities are mainly a result of excessive overlaps, improper positioning of carcass strips, steel and cap plies, as well as the incorrect formation of tread material. The authors further stated that these non-uniformity defects are practically impossible to detect with human sensory detection methods, and this increase the risks of having defective tyres on the road. Hence, the process of tyre inspection during production needs to be optimised by minimising the need for human intervention which may also be associated with errors while conducting a visual inspection, and one promising approach that is currently being experimented with by researchers for predictive modelling is by the use of artificial neural networks.

In this study, the performance of transfer learning using a pre-trained convolutional neural network (CNN) [18] – [23] which includes ResNet-50 and VGG-19 for feature extraction [24], combined with other machine learning algorithms that include Random-forest (RF), Logistic regression (LR), and Support Vector Machine (SVM) was inquired for the final identification and classification of a good and defective tyre.

The rest of this paper is arranged as follows. Section 2 presents the related works, while Section 3 presents the methodology employed to do this work. Section 4 shows the evaluation of the performance of the models, while Section 5 offers the discussion. Finally, Section 6 concludes the paper.

II. RELATED WORKS

Over the years, studies on tyre defect detection have become significant. Several experiments have been conducted on optimising inspection and quality control of tyres during production and while they are in service [25]. Some of the investigations include the incorporation of an algorithm that is based on Fourier transform on a real-time X-ray system for defects detection [26], and holographic non-destructive testing in which the material to be tested is subjected to stress that is uniformly distributed across its surface, to study the behaviour using holographic interferometry to spot the defect which is then visualised in the form of inferences superimposed on the surface of the material [27] – [29].

Zhang et al. [15] conducted a study using edge-detection approaches for defect detection in tyres. In their research, a curvelet-based improved Canny edge detection scheme was implemented to detect defective edges in tyre laser shearography images by identifying the point of discontinuity in the tyre images. The authors noted that it is difficult to design a general edge detection algorithm that performs well in many contexts and captures the requirements of subsequent processing stages, however, their findings suggest that their method outperforms the conventional Canny, Sobel, and LoG edge detection methods in detecting accuracy of the edge of interference fringe.

The past decades have recorded remarkable successes in the use of representation learning for object recognition and classification [30], [31], and this has induced increased research in the use of CNN methods for the optimisation of quality control. Wang et al. [32] conducted a study in which they proposed a tyre detection method based on a fully convolutional network (FCN), taking advantage of the powerful self-learning and segmentation capability of FCN to overcome the deficiency of the traditional tyre defect detection. Their experiment simplified the full convolution segmentation network into binary classification and pixel-wise prediction models and combined different scale features to refine the defection results. They then compared VGGNet with the configurations and depths of VGG11, VGG13, and VGG16, used a two-dimensional interpolation strategy for obtaining the enlarged feature map, and compared the results of their experiments with traditional methods. They obtained results that showed that their approach provides more applicability to many types of defects than the traditional method.

In an experiment conducted by Kuric et al. [5], the authors proposed a method that processes tyre sidewall data comprising both visual and geometric data characterising the surface of the tyre. In their study, the authors utilised 12 Mpx monochrome industrial cameras to obtain visual characteristics of the tyre sidewall. They identified the geometry and abnormalities of the tyre sidewall by a laser sensor. They further used an unsupervised clustering method, followed by the classification of defects using the VGG-16 neural network, and obtained over 94% defect-recognition accuracy, when this approach was used for the classification of abnormalities of tyre sidewall.

Li et al. [4], proposed a TyreNet model that used an end-to-end method for automatic tyre defect detection and used a model that focused on learning the features of the good tyre images rather than defective images. Their experiment used the X-ray image output of the tyre from X-ray machines as their original dataset. During data preprocessing, the authors processed 120,000 images consisting of 100,000 good tyres and 20,000 defectives into a total of 480,000 sub-images, and to improve the image recognition quality, they further cut the image size from (3,456, 22,000) to several sub-images with size (900, 900). Their final result showed that their proposed TyreNet method with ResNet-50 backbone outperformed the other methods (SSD512, YOLOv3, and Faster R-CNN) they compared with their work.

In recent times, methods that involve a combination of ANNs with other machine learning algorithms have been applied by researchers to optimise the performance of deep learning, and also domain adaptation methods have been used for solving cross-domain defect detection problems [13], [33]. Lin [34] experimented to improve the traditional ShuffleNet for tyre crack detection. The author then compared their findings with five methods including GoogLeNet, traditional ShuffleNet, VGGNet, ResNet, and improved ShuffleNet through tyre database verification. Their results showed that the improved Shufflenet method achieved the highest accuracy of 94.7%, compared to GoogleNet, Traditional Shufflenet, VGGNet, and ResNet.

In another experiment conducted by Liu et al [34], they studied tyre appearance defect detection using a method that combines a histogram of oriented gradients (HOG) and local binary pattern (LBP) features. In their experiment, they constructed a tyre image dataset to provide defective and normal tyre images, histogram of oriented gradients and local binary pattern features of tyre images were extracted respectively and used to train the support vector machine (SVM) classifier to get the prediction probability values for feature fusion and then compared the result of combining the algorithm HOG + SVM, LBP + SVM, and HOG + LBP + SVM. Their experimental results showed that HOG + SVM has an accuracy of 70%, LBP + SVM have an accuracy of 82%, and HOG + LBP + SVM provides the highest accuracy of 84%. Zheng et al [35] attempted to address problems associated with intelligent tyre defect detection using an end-to-end saliency detection network by proposing a novel two-stage convolutional neural network and an end-to-end residual U-structure (HLU2-Net) for tyre defect detection.

Literature suggests that deep learning-based methods have demonstrated promising results in tyre defect detection. However, the performance of these models depends very much on the availability of large training data, whereas, the availability of defective tyre data sets is limited. Also, though the previous works suggest that deep learning algorithms may be more suitable as the basic method for virtual defect detection of tyres, the works have not yet achieved the application-level requirements. Motivated by previous works on the identification of tyre defects using deep learning methods, the authors conduct this study to compare the performance of pre-trained CNN combined with various traditional ML algorithms for visual tyre defect detection.

III. METHODOLOGY

In this study, we explored the performance of transfer learning using a pre-trained convolutional neural network (CNN) for feature extraction, combined with other machine learning algorithms for the final classification of tyre defects. This hybrid approach allows us to leverage the deep feature representations extracted by ResNet50 and VGG19 [24] while also capitalising on the strengths of traditional machine learning algorithms (SVM, RF, and LR) for robust predictive modelling. The features extracted by these CNNs respectively were combined with the other ML algorithms by exploring various fusion techniques to effectively integrate the features. We then fine-tune the hyperparameters and conduct cross-validation to optimise the model performance.

A. Theoretical Framework

An artificial neural network (ANN) is a computational model that is inspired by how the human brain is structured, and also how it functions. It consists of a network of interconnected artificial neurons that operate in tandem to learn and recognise patterns [29]. These neurons are organised into layers and learn to perform specific tasks by adjusting the strength of connections between neurons based on input data. Each neuron consists of connections of nodes which receive the inputs (x), weight (w) for the corresponding signals, and the bias (b). The connection of these neurons is associated with weight and applies an activation function (f) to its input. ANNs process data through feedforward propagation, where inputs move from the input layer through the hidden layers to the output layer, and training is carried out by backpropagation, which involves adjusting the weights and biases to minimise the loss function. The neuron can be described with a transfer function according to (1) below.

$$y = f(w^T x + b) \tag{1}$$

During its operation, each neuron receives signals from other neurons, processes the input signals, and outputs a processed signal to other neurons. One of the earliest and most influential ANNs is the perceptron, proposed by Frank Rosenblatt in 1958 [37]. It is a single-layer neural network that can classify linearly separable input data by adjusting the weights of its inputs. However, the perceptron has a limited ability to handle more complex input data, leading to the development of multi-layer neural networks [38], such as the convolutional neural network (CNN). ANNs usually require large amounts of training datasets, where the input data is fed into the network and the network learns by modifying its parameters to minimise the error between the predicted output (y) and the correct output (d), via a process known as backpropagation [39], which involves propagating the error signal back through the network to adjust the weights and biases of the neurons [40].

For a neural network that consists of two input nodes ($x_1 and\ x_2$) and two output nodes ($y_1 and\ y_2$), with a hidden layer and an activation function (φ). To obtain the output error, first, we calculate the weighted sum (w) of the hidden node using the equation $v = wx + b$ and calculate the output (y) by putting the weighted sum into the activation function (φ) as expressed by the equation $y = \varphi(v) = \varphi(wx + b)$. To train the neural network using the back-propagation algorithm, the hidden layer errors (e) are determined from the expressed as $e_n = d_n - y_n$, and the delta rule (δ) is applied, given as $\delta_n = \varphi'(v_n)e_n$. Where φ' is the derivative of the activation function. In the back-propagation algorithm, the error of the node is obtained from the weighted sum of the back-propagation deltas of the output layer. This is expressed as follows

$$e_1^1 = w_{11}^2\delta_1 + w_{21}^2\delta_2 \tag{2}$$

$$e_2^1 = w_{12}^2\delta_1 + w_{22}^2\delta_2 \tag{3}$$

Combining (2) and (3), we obtain (4)

$$\begin{bmatrix} e_1^1 \\ e_2^1 \end{bmatrix} = W_2^T \begin{bmatrix} \delta_2 \\ \delta_2 \end{bmatrix} \tag{4}$$

This backward process is repeated for all hidden layers to calculate the deltas, and train the neural network with the learning rate α (where $0 < \alpha \leq 1$). Training the neural network using the backpropagation algorithm requires the following steps [39].

Step 1: Initialize the weights with the required values.

Step 2: Enter the input from the training data {input, correct output} and obtain the neural network's output.

Step 3: Calculate the layer's error, and the delta, δ, of the output nodes.

$$e = d - y$$

$$\delta = \varphi'(v)e$$

Step 4: Propagate the output node delta, δ, backwards, and calculate the deltas of the immediate next (left) nodes.

$$e^{(k)} = W^T\delta$$

$$\delta^{(k)} = \varphi'(v^k)e^k$$

Step 5: Repeat Step 4 until it reaches the hidden layer that is on the immediate right of the input layer.

Step 6: Adjust the weights according to the learning rule:

$$\Delta W_{ij} = \alpha\delta_i x_j$$

$$W_{ij} \leftarrow W_{ij} + \Delta W_{ij}$$

Step 7: Repeat Steps 2-6 for every training data point.

Step 8: Repeat Steps 2-6 until the neural network is appropriately trained.

B. Research Design

The study starts with data collection followed by the data preparation stage which involves data Pre-processing which is crucial for data quality enhancement, and includes image resizing, normalization and splitting data into training sets and validation sets to create a consistent and reliable dataset. The next stage is Feature extraction carried out to extract essential features from the images using the ResNet50 and VGG19 pre-trained CNN respectively to capture critical patterns and structures. This was followed by a Model Training operation where the extracted features were used to train a range of ML algorithms, including LR, RF, and SVM, and each of the algorithms was carefully tuned and trained to optimise their performance. The final stage is the model evaluation stage, where various metrics and validation techniques are used to assess the performance of the models. *Figure 1* below depicts the project's workflow, with an illustration of the key stages of the process.

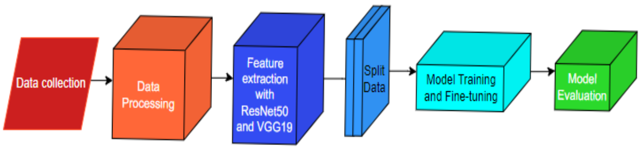

Figure 1: Pipeline Overview

1) Data description: The data used for this study was obtained from the Mendeley defective tyre dataset, which can be found here https://data.mendeley.com/datasets/bn7ch8tvyp/1. It consisting of 1854 digital images was used in this experiment to analyze the condition of tyres. The images of the tyres were meticulously labelled and categorized into 'defective' and 'in good condition' classes.


Figure 2: Defective tyre images (left) and good tyre images (right)

While performing exploratory data analysis, we observed the data was collected across various vehicle categories to ensure high-quality imagery, and the dataset contains 1028 images of defective tyres and 828 images of good tyres. The nature of the defects include irregular tread wear, bulges, cracks, cuts and punctures, tread separation, tread-deformation, and blowout [10].

2) System Architecture: The study uses ResNet50 and VGG19 pre-trained models for feature extraction and machine learning algorithms like LR, RF, and SVM for predictive analysis. ResNet50 extracts 51,200 features, while VGG19 captures localised and fundamental features at 8,192. ResNet50 is ideal for high-accuracy tasks and computational resources, while VGG19 balances accuracy and efficiency for real-time processing or resource limitations.

a) ResNet50: This is a deep convolutional neural network architecture with 50 layers, utilising residual connections to address vanishing gradient problems during training. It uses a fixed-size input image, convolutional layers, and 16 residual blocks. ResNet-50 uses Global Average Pooling (GAP) to reduce spatial dimensions and has

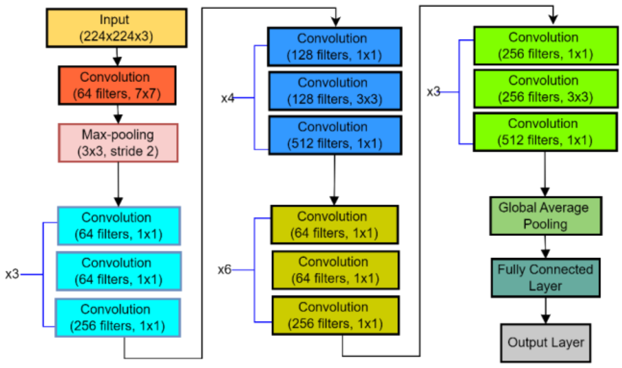

Figure3:ResNet50 Architecture

a fully connected layer with many neurons for classification tasks. These connections make training deep networks easier and improve gradient flow during backpropagation. It also has a final output layer that computes class probabilities for image classification tasks [41].

b) VGG19: This is a deep convolutional neural network architecture used for image classification, which is part of the VGG series developed by the University of Oxford. It consists of 19 layers, including 16 convolutional and three fully connected layers, with a filter size of 3 × 3 [41].

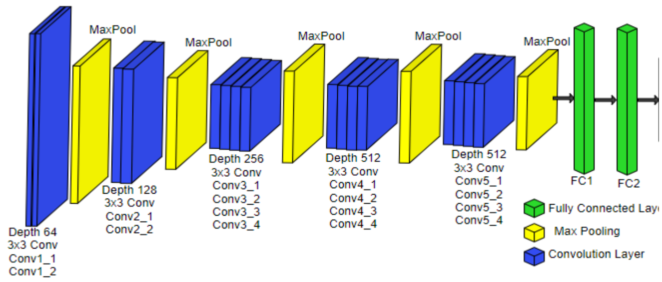

Figure 4: VGG19 Architecture

IV. PRESENTATION OF RESULTS

In this section, we evaluated the performance of ResNet50 + LR, ResNet50 + RF, ResNet50 + SVM, VGG19 + LR, VGG19 + RF, and VGG19 + SVM respectively. Table 1 contains the confusion matrix results, which show that the number of tyres correctly classified by ResNet50 + LR as defective and good respectively are 176 and 130, while the wrongly classified cases as defective and good respectively are 36 and 30. The number of tyres correctly classified by ResNet50 + RF as defective and good are 182 and 112, while the cases wrongly classified as defective and good respectively are 54 and 24. The number of tyres correctly classified by ResNet50 + SVM as defective and good respectively are 170 and 127, while the cases wrongly classified as defective and good respectively are 39 and 36. The numbers of tyres correctly classified by VGG19 + LR as defective and good are 179 and 139 respectively, while 27 cases were classified respectively as defective and good. The number of cases correctly classified by VGG19 + RF defective and good are 178 and 130 respectively, while the number of cases wrongly classified as defective and good respectively are 36 and 28. Finally, the number of cases classified by VGG19 + SVM as defective and good respectively are 180 and 138, while the number of cases wrongly classified as defective and good are 28 and 26.

TABLE 1: CONFUSION MATRIX RESULTS

Models	TP	FP	TN	FN
ResNet50 + LR	176	36	130	30
ResNet50 + RF	182	54	112	24
ResNet50 + SVM	170	39	127	36
VGG19 + LR	**179**	**27**	**139**	**27**
VGG19 + RF	178	36	130	28
VGG19 + SVM	**180**	**28**	**138**	**26**

Table 1 shows that for the models in which the traditional ML algorithms were combined with ResNet50, ResNet50 + RF had the highest cases of TP, while ResNet50 + SVM had the lowest cases. For the numbers of TN obtained, Resnet50 + RF had the lowest while ResNe50 + LR had the highest. Meanwhile, ResNet50 + RF had the highest cases of FP and also the lowest cases of FN.

V. DISCUSSION

The application of deep learning for the identification and classification of good and defective tyres was explored in this study. The performance of transfer learning using pre-trained CNN that includes ResNet-50 and VGG-19 for feature extraction, combined with RF, LR, and SVM for the final classification was explored. *Table 2 and 3* provide a summary of the training and validation Accuracy (Acc), Precision (Preci), Recall and F1-score (F1) for the different machine learning models used in this study, with each combining a specific feature extractor (ResNet50 or VGG19) with one of three classifiers (LR, RF, or SVM).

A. Training Result For The Machine Learning Algorithms

From Table 2 below, we observed that VGG19 + SVM outperforms all the other models in their accuracy, precision, recall, and F1 score. The highest accuracy was obtained by VGG19 + SVM at 97.24%, followed by VGG19 + RF with an accuracy of 95.1%. The lowest accuracy was obtained by ResNet50 + SVM at 90.36%. This indicates that the VGG19 features, when processed with SVM, are highly effective at classifying the data during the training phase, while Resnet50 + SVM performance at the training phase is lowest compared to all the other models.

TABLE 2: TRAINING RESULT FOR THE MACHINE LEARNING ALGORITHMS

Models	Acc (%)	Preci (%)	Recall (%)	F1 (%)
ResNet50 + LR	94.47	94.48	94.47	94.46
ResNet50 + RF	92.39	92.71	92.39	92.33
ResNet50+SVM	90.36	90.36	90.36	90.36
VGG19 + LR	94	94.03	94	94.01
VGG19 + RF	95.01	95.02	95.01	95.01
VGG19 + SVM	**97.24**	**97.25**	**97.24**	**97.24**

B. Validation Results For The Machine Learning Algorithms:

Table 3 indicates that VGG19 + LR achieved the highest performance with accuracy, precision, recall and F1-score of 85.48%. VGG19 + SVM also maintain high performance with an accuracy and recall of 85.48%, and a precision and F1-score of 85.47% respectively. However, when we compared the results of Tables 2 and 3, we found that some level of consistency exists in the performance of the models between training and validation, indicating that overfitting was effectively managed. Furthermore, the results show that all the models exhibited a slight decrease in performance when moving from training to validation, which is a common trend due to the model's adaptation to the training dataset. Finally, the results in Figure 17 indicate that the chosen combinations have a good balance between accuracy, precision, recall, and F1-score.

TABLE 3: VALIDATION RESULT FOR THE MACHINE LEARNING ALGORITHMS

Models	Acc (%)	Preci (%)	Recall (%)	F1 (%)
ResNet50 + LR	82.26	82.23	82.26	82.22
ResNet50 + RF	79.03	79.45	79.03	78.7
ResNet50 + SVM	79.84	79.81	79.84	79.82
VGG19 + LR	**85.48**	**85.48**	**85.48**	**85.48**
VGG19 + RF	82.8	82.78	82.8	82.75
VGG19 + SVM	**85.48**	**85.47**	**85.48**	**85.47**

C. Benchmarking Of Our Experimental Result With The Result Obtained By Liu et al. [12].

In the experiment conducted by Liu et al. [12] on tyre appearance defect detection, they combined histogram of oriented gradients (HOG) and local binary pattern (LBP) features with other algorithms HOG + SVM, LBP + SVM, and HOG + LBP + SVM, their experimental results showed that HOG + SVM have an accuracy of 70%, LBP + SVM have an accuracy of 82%, while HOG + LBP + SVM have the highest accuracy of 84%.

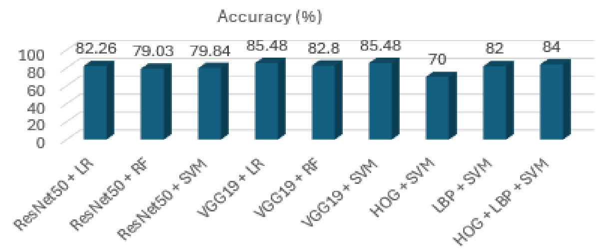

Figure 5: Benchmark of the accuracy of different models

However, when we compared the result of their study with the findings of our experiment as shown in Figure 5 above, it was observed that VGG19+LR and VGG19 +SVM achieved a slightly higher accuracy of 1.48% above their model HOB+LBP+SVM which has the highest accuracy. This inferred that both the VGG19+LR and VGG19 +SVM methods achieved a slight improvement in the performance for visual tyre defect classification when compared to the approach used in the study conducted by Liu et al. [12].

VI. CONCLUSION

The results of our experiment as shown in Table 3 indicated that combining VGG19 with LR, and RF respectively, consistently outperforms the other models. The ResNet50 + LR model also performs well on the training data. VGG19 + SVM shows the highest accuracy, precision, recall, and F1 score among all the combinations, with an impressive accuracy of 97.24%.

This indicates that the VGG19 features, when processed with SVM, are highly effective at classifying the data during the training phase. For all the models, we observed that for the TP, the ResNet50 + RF model stands out with the highest instances of 182, followed closely by VGG19 + RF and VGG19 + SVM models. For the FP, VGG19 + LR model has the lowest instance 27, followed by VGG19 + SVM which has 28 instances. The number of instances of TN for "VGG19 + LR" was 139, closely followed by "VGG19 + SVM" which had 138 instances. Finally, for the FN, ResNet50 + RF had the lowest instance of 24, closely followed by “VGG19 + SVM” which has 26 instances.

Hence, the study indicates that the VGG19 feature extractor, combined with LR and SVM respectively, provides a promising solution to the problem associated with automating tyre quality control processes, and aims to advance the state-of-the-art defect detection systems during tyre production, thereby contributing to the general safety and efficiency of the automobile industry.

This study was limited to the classification of tyres into good and defective based on the identified surface defect. However, the immediate next research steps should be to explore the identification of internal defects and the time to failure of tyres in operations.

REFERENCES

[1] Erdogan, S. (2009). Explorative spatial analysis of traffic accident statistics and road mortality among the provinces of Turkey. Journal of safety research, 40(5), 341-351, https://doi.org/10.1016/j.jsr.2009.07.006

[2] Zheng, Z., Zhang, S., Yu, B., Li, Q., & Zhang, Y. (2020). Defect inspection in tire radiographic image using concise semantic segmentation. Ieee Access, 8, 112674-112687, https://doi.org/10.1109/ACCESS.2020.3003089

[3] Yang, H., Jiang, Y., Deng, F., Mu, Y., Zhong, Y., & Jiao, D. (2022). Detection of Bubble Defects on Tire Surface Based on Line Laser and Machine Vision. Processes, 10(2), 255, https://doi.org/10.3390/pr10020255

[4] Li, Y., Fan, B., Zhang, W., & Jiang, Z. (2021). TireNet: A high recall rate method for practical application of tire defect type classification. Future Generation Computer Systems, 125, 1-9, https://doi.org/10.1016/j.future.2021.06.009

[5] Kuric, I., Klarák, J., Sága, M., Císar, M., Hajdučík, A., & Wiecek, D. (2021). Analysis of the possibilities of tire-defect inspection based on unsupervised learning and deep learning. Sensors, 21(21), 7073, https://doi.org/10.3390/s21217073

[6] West, W. J., & Limebeer, D. J. (2020). Optimal tyre management of a formula one car. IFAC-PapersOnLine, 53(2), 14456-14461, https://doi.org/10.1016/j.ifacol.2020.12.1446

[7] Gehrke, I., Schläfle, S., Bertling, R., Öz, M., & Gregory, K. (2023). Mitigation measures to reduce tire and road wear particles. Science of The Total Environment, 166537, https://doi.org/10.1016/j.scitotenv.2023.166537

[8] Xing, K., Cheng, P., Wang, Q., & Li, H. (2024). Optimal design of radial tire section layout based on thermal fatigue life improving. Heliyon, 10(1), https://doi.org/10.1016/j.heliyon.2023.e22864

[9] Guo, Q., Zhang, C., Liu, H., & Zhang, X. (2016). Defect detection in tire X-ray images using weighted texture dissimilarity. Journal of sensors, 2016, https://doi.org/10.1155/2016/4140175

[10] Weyssenhoff, A., Opala, M., Koziak, S., & Melnik, R. (2019). Characteristics and investigation of selected manufacturing defects of passenger car tires. Transportation research procedia, 40, 119-126. https://doi.org/10.1016/j.trpro.2019.07.020

[11] Yang, S., Jiao, D., Wang, T., & He, Y. (2022). Tire speckle interference bubble defect detection based on improved faster RCNN-FPN. Sensors, 22(10), 3907. https://doi.org/10.3390/s22103907

[12] Liu, H., Jia, X., Su, C., Yang, H., & Li, C. (2023). Tire appearance defect detection method via combining HOG and LBP features. Frontiers in Physics, 10, 1099261. https://doi.org/10.3389/fphy.2022.1099261

[13] Zhang, Y., Wang, Y., Jiang, Z., Zheng, L., Chen, J., & Lu, J. (2023). Domain adaptation via Transferable Swin Transformer for tire defect detection. Engineering Applications of Artificial Intelligence, 122, 106109. https://doi.org/10.1016/j.engappai.2023.106109

[14] Abou-Ali, M. G., & Khamis, M. (2003). TIREDDX: an integrated intelligent defects diagnostic system for tyre production and service. Expert Systems with Applications, 24(3), 247-259. https://doi.org/10.1016/S0957-4174(02)00153-7

[15] Zhang, Y., Li, T., & Li, Q. (2013). Defect detection for tire laser shearography image using curvelet transform based edge detector. Optics & Laser Technology, 47, 64-71. https://doi.org/10.1016/j.optlastec.2012.08.023

[16] Vincent, O. R., Babalola, Y. E., Sodiya, A. S., & Adeniran, O. J. (2021). A Cognitive Rail Track Breakage Detection System Using Artificial Neural Network. Applied Computer Systems, 26(2), 80-86. https://doi.org/10.2478/acss-2021-0010

[17] Katsigiannis, S., Seyedzadeh, S., Agapiou, A., & Ramzan, N. (2023). Deep learning for crack detection on masonry façades using limited data and transfer learning. Journal of Building Engineering, 107105. https://doi.org/10.1016/j.jobe.2023.107105

[18] Barbero-Aparicio, J. A., Olivares-Gil, A., Rodríguez, J. J., García-Osorio, C., & Díez-Pastor, J. F. (2024). Addressing data scarcity in protein fitness landscape analysis: A study on semi-supervised and deep transfer learning techniques. Information Fusion, 102, 102035. https://doi.org/10.1016/j.inffus.2023.102035

[19] Dais, D., Bal, I. E., Smyrou, E., & Sarhosis, V. (2021). Automatic crack classification and segmentation on masonry surfaces using convolutional neural networks and transfer learning. Automation in Construction, 125, 103606. https://doi.org/10.1016/j.autcon.2021.103606

[20] .Guo, Y., Gao, C., Jin, Y., Li, Y., Wang, J., Li, Q., & Wang, H. (2023). A transfer learning-based method for marine machinery diagnosis with small samples in noisy environments. Journal of Ocean Engineering and Science. https://doi.org/10.1016/j.joes.2023.12.004

[21] Sadik, R., Majumder, A., Biswas, A. A., Ahammad, B., & Rahman, M. M. (2023). An in-depth analysis of Convolutional Neural Network architectures with transfer learning for skin disease diagnosis. Healthcare Analytics, 3, 100143. https://doi.org/10.1016/j.health.2023.100143

[22] Wu, X., Manton, J. H., Aickelin, U., & Zhu, J. (2023). A Bayesian approach to (online) transfer learning: Theory and algorithms. Artificial Intelligence, 324, 103991. https://doi.org/10.1016/j.artint.2023.103991

[23] Banda, P., Bhuiyan, M. A., Hasan, K. N., & Zhang, K. (2023). Assessment of hybrid transfer learning method for forecasting EV profile and system voltage using limited EV charging data. Sustainable Energy, Grids and Networks, 36, 101191. https://doi.org/10.1016/j.segan.2023.101191

[24] Ikechukwu, A. V., Murali, S., Deepu, R., & Shivamurthy, R. C. (2021). ResNet-50 vs VGG-19 vs training from scratch: A comparative analysis of the segmentation and classification of Pneumonia from chest X-ray images. Global Transitions Proceedings, 2(2), 375-381. https://doi.org/10.1016/j.gltp.2021.08.027

[25] Zhang, Y., Cui, X., Liu, Y., & Yu, B. (2018). Tire defects classification using convolution architecture for fast feature embedding. International Journal of Computational Intelligence Systems, 11(1), 1056-1066. https://doi.org/10.2991/ijcis.11.1.80

[26] Gayer, A., & Saya, A. (1988). The use of X-radiography and computer software for detecting defects during the manufacture of steel-belt tyres. NDT International, 21(5), 333-336. https://doi.org/10.1016/0308-9126(88)90192-7

[27] Grant, R. and Brown, G, (1969). Holographic Nondestructive Testing (HNDT) in the Automotive Industry. SAE Transactions, 78, 305–313. http://www.jstor.org/stable/44563012

[28] Borza, D. N. (1998). Specialized techniques in holographic non-destructive testing of composites. Composites Part B: Engineering, 29(4), 497-504. https://doi.org/10.1016/S1359-8368(98)00006-7

[29] Ganesan, A. R. (2009, December). Holographic and laser speckle methods in non-destructive testing. In Proceedings of the National Seminar & Exhibition on Non-Destructive Evaluation (pp. 126-130).

[30] Bengio, Y., Courville, A., & Vincent, P. (2013). Representation learning: A review and new perspectives. IEEE transactions on pattern analysis and machine intelligence, 35(8), 1798-1828. https://doi.org/10.48550/arXiv.1206.5538

[31] Adenusi, C. A., Vincent, O. R., Abodunrin, J., & Adebiyi, B. T. (2022). COVID-19 Face Mask Detection Using CNN and Transfer Learning. In Decision Sciences for COVID-19: Learning Through Case Studies (pp. 393-405). https://doi.org/10.1007/978-3-030-87019-5_22

[32] Wang, R., Guo, Q., Lu, S., & Zhang, C. (2019). Tire defect detection using fully convolutional network. IEEE Access, 7, 43502-43510. https://doi.org/10.1109/ACCESS.2019.2908483

[33] Abdallah, T. B., Elleuch, I., & Guermazi, R. (2021). Student behaviour recognition in the classroom using deep transfer learning with VGG-16. Procedia Computer Science, 192, 951-960. https://doi.org/10.1016/j.procs.2021.08.098

[34] Lin, S. L. (2023). Research on tire crack detection using image deep learning method. Scientific Reports, 13(1), 8027

[35] Zheng, Z., Yang, H., Zhou, L., Yu, B., & Zhang, Y. (2021). HLU 2-Net: a residual U-structure embedded U-Net with hybrid loss for tire defect inspection. IEEE Transactions on Instrumentation and Measurement, 70, 1-11. https://doi.org/10.1109/TIM.2021.3126847

[36] Pérez-Gomariz, M., López-Gómez, A., & Cerdán-Cartagena, F. (2023). Artificial neural networks as artificial intelligence technique for energy saving in refrigeration systems—A review. Clean Technologies, 5(1), 116-136. https://doi.org/10.3390/cleantechnol5010007

[37] Rosenblatt, F. (1958). The perceptron: a probabilistic model for information storage and organization in the brain. Psychological review, 65(6), 386. https://doi.org/10.1037/H0042519

[38] Rumelhart, D. E., Hinton, G. E., & Williams, R. J. (1986). Learning representations by back-propagating errors. nature, 323(6088), 533-536. https://doi.org/10.1038/323533a0

[39] Phil, K. (2017). Matlab deep learning with machine learning, neural networks and artificial intelligence. Apress, New York. https://doi.org/10.1007/978-1-4842-2845-6

[40] Mohammadazadeh, A., Sabzalian, M. H., Castillo, O., Sakthivel, R., El-Sousy, F. F., & Mobayen, S. (2022). Neural Networks and Learning Algorithms in MATLAB. Springer Nature. https://doi.org/10.1007/978-3-031-14571-1

[41] Ali, L., Alnajjar, F., Jassmi, H. A., Gocho, M., Khan, W., & Serhani, M. A. (2021). Performance evaluation of deep CNN-based crack detection and localization techniques for concrete structures. Sensors, 21(5), 1688. https://doi.org/10.3390/s21051688